High-speed InGaAsP electroabsorption modulators: dependence of the device characteristics on the mesa design

G. E. Shtengel
Lucent Technologies, Bell Laboratories, 9999 Hamilton blvd., Breinigsville, PA 18031
voice: +1 (610) 391 2718, FAX: +1 (610) 391 2185, e-mail: gleb@lucent.com

A .E. Bond
Lucent Technologies, Bell Laboratories, 9999 Hamilton blvd., Breinigsville, PA 18031
voice: +1 (610) 391 2351, FAX: +1 (610) 391 2434, e-mail: abond1@lucent.com

Y. A. Akulova
Lucent Technologies, Bell Laboratories, 9999 Hamilton blvd., Breinigsville, PA 18031
voice: +1 (610) 391 2914, FAX: +1 (610) 391 2434, e-mail: yakulova@lucent.com

C. L. Reynolds, Jr.
Lucent Technologies, Bell Laboratories, 9999 Hamilton blvd., Breinigsville, PA 18031
voice: +1 (610) 391 2587, FAX: +1 (610) 391 2434, e-mail: lr@lucent.com

We present characteristics of InGaAsP electroabsorption modulators with variable length and mesa width. We demonstrate devices with return loss below -10dB, bandwidth above 40GHz and extinction ratio of 10dB/2V. We show that low capacitance is advantageous for high-speed operation even when achieved at the expense of increased series resistance.

High-speed InGaAsP electroabsorption modulators: dependence of the device characteristics on the mesa design

G. E. Shtengel
Lucent Technologies, Bell Laboratories, 9999 Hamilton blvd., Breinigsville, PA 18031
voice: +1 (610) 391 2718, FAX: +1 (610) 391 2185, e-mail: gleb@lucent.com

A .E. Bond
Lucent Technologies, Bell Laboratories, 9999 Hamilton blvd., Breinigsville, PA 18031
voice: +1 (610) 391 2351, FAX: +1 (610) 391 2434, e-mail: abond1@lucent.com

Y. A. Akulova
Lucent Technologies, Bell Laboratories, 9999 Hamilton blvd., Breinigsville, PA 18031
voice: +1 (610) 391 2914, FAX: +1 (610) 391 2434, e-mail: yakulova@lucent.com

C. L. Reynolds, Jr.
Lucent Technologies, Bell Laboratories, 9999 Hamilton blvd., Breinigsville, PA 18031
voice: +1 (610) 391 2587, FAX: +1 (610) 391 2434, e-mail: lr@lucent.com

1. Introduction

The fast increase of the bit-rate of the optical fiber communications imposes stringent requirements on components such as transmitters. $LiNbO_3$ Mach-Zehnder (MZ) modulators as well as electroabsorption (EA) modulators are being considered. The requirements include high modulation bandwidth, high extinction ratio, low electrical return loss, and high saturation power. Polarization sensitivity might also be an issue if device is used at the receiver end. Another important requirement is low drive voltage. EA modulators have the advantage of lower drive voltage and it is critical at 40Gb/s bit rates.

EA devices with multi-quantum well (MQW) active layers utilize a combination of the quantum-confined Stark effect and the Franz-Keldysh effect, and therefore offer higher extinction ratios than bulk EA modulators. However MQW structures might present problems caused by carrier escape and transport through MQW layers which can decrease the modulation bandwidth and reduce the saturation power.

There have been a number of reports on the realization of EA modulators with a modulation bandwidth in excess of 40GHz in the InGaAlAs material [1] as well as in the InGaAsP system [2]. The EA section of the device is kept short to minimize the device capacitance (in most of the reports it is of an order of 100μm). To keep the extinction ratio high, the number of quantum wells is typically increased to 15-20. This also results in the increased thickness of the undoped layer and therefore further reduces the device capacitance. However, devices with such short EA sections cannot be used for practical purposes. Handling such devices is complicated, and stray light degrades the extinction ratio. Placing the EA section between two passive waveguide sections increases the device length. Using the beam-expanders as passive sections also allows for improvement of optical coupling [3].

2. Device Structure

The schematic of the device structure is shown in Fig.1. The InGaAsP EA modulators were grown on a n+(100) InP substrate in a low-pressure MOVPE system. The MQW structure is overall strain-compensated and consists of 18 quantum wells. Beam-expander sections were fabricated using butt-joint technology: the MQW layers were selectively etched and regrown with bulk quaternary layer to form the passive waveguide. The entire surface of the wafer was then capped with a thick p-InP cladding layer and a heavily doped p+-InGaAs contact layer. The waveguides were fabricated in a reactive ion etching (RIE) system based on a CH_4/H_2 etch chemistry. After the waveguide formation the devices were planarized

using polyimide and p- and n- contacts were deposited. Use of the thick polyimide layer reduces parasitic capacitance in the device (blocking structure capacitance and contact pad capacitance).

2. Device results.

The devices were mounted p-up on submounts with a coplanar electrical waveguide and an integrated matching 50Ω resistor, allowing for high-speed probing with ground-signal-ground probes. We characterized 2 sets of devices with different lengths of the EA sections: 80μm and 120 μm. The total length of the device, including the beam-expander sections, was 600 μm for all devices. Within each set of devices, the mesa width varied from 1.4 to 2.8 μm (the mesa width is constant along the entire length of the device). We performed DC Extinction measurements as well as high-speed S-parameter characterization. Devices with shorter cavities have lower extinction, but higher small-signal bandwidth and lower electrical return loss. Fiber-to-fiber insertion loss was between 10 and 18dB for most of the devices and was due to facet quality. We did not observe any dependence on the mesa width or active layer length.

A set of DC extinction curves for device with 120μm long EA section and mesa width of 1.4μm is shown in Fig.2. The DC extinction between -1 and -3V is 10dB. This value is independent of mesa width.

We used an HP8510C Network Analyzer and an HP84330D p-i-n detector to perform the S-parameter measurements. The calibration of the HP84330D detector is accurate only up to ~35GHz. More than half of the devises tested had bandwidth exceeding this value, in this case it is reported as 40GHz.

Shown in Fig.3 is the set of small-signal response (S_{21}) curves for the device in Fig.2 (120μm long EA section and mesa width of 1.6μm), taken at different DC biases. The 3dB bandwidth increases with negative DC bias because the capacitance of reverse-biased p-n junction decreases as the reverse bias increases. At -2V the 3dB bandwidth exceeds 35GHz.

The value of 3dB bandwidth at -2V of DC bias as a function of mesa width for devices with 80μm and 120μm EA sections is plotted in Fig.5. It is known that in order to optimize the EA performance one needs to reduce both series resistance and device capacitance. The series resistance of the EA's is inversely proportional to the mesa area of the device, so it decreases as the mesa width increases. However the device capacitance is proportional to the mesa area, so it increases as the mesa width increases. The 3dB bandwidth of 120μm long devices decreases as the mesa width increases, and the bandwidth of all but one 80μm long device exceeds 35GHz. This trend indicates that for higher modulation bandwidth the low device capacitance is most important, even if achieved at the expense of increased series resistance. These very high values of bandwidths also allow for conclusion that the carrier transport effects do not limit the device performance.

Electrical return loss (S_{11}) as a function of frequency at different DC biases is plotted in Fig.4 (for the EA device in Figs. 2 and 3). The shape of the S_{11} curve is characteristic of the RC equivalent circuit. The amplitude of S_{11} increases with frequency up to 20GHz, and does not change much between 20 and 40GHz. The value of S_{11} at 20GHz and at -1V of DC bias is plotted in Fig.6 as a function of the mesa width for devices with 80μm and 120μm EA sections. The devices with smaller mesas have higher series resistance and lower capacitance. Both effects contribute to reduction of the electrical return loss.

We have studied the set of devices with varying mesa width and length of the EA section. We observed no dependence of fiber-to-fiber insertion loss on the mesa width. The devices with narrower mesas have higher modulation bandwidth and lower electrical return loss. This indicates that the smaller device capacitance is advantageous for high-speed operation, even when achieved at the expense of increased series resistance.

We would like to thank Ron Leibenguth, George Przybylek, Ken Glogovsky, and Brian Falk for their help in the device fabrication.

3. References.

1. K. Wakita et al, *IEICE Trans. Electron.,* Vol. E81-C, No. 2, pp. 175-79, 1998.
2. Satzke, et al, *Electron. Lett.,* Vol. 31, No. 23, pp. 2030-32, 1995.
3. T. Ido, et al, *IEEE Photon. Technol. Lett.,* vol.7, No. 2, pp.170-172, 1995.

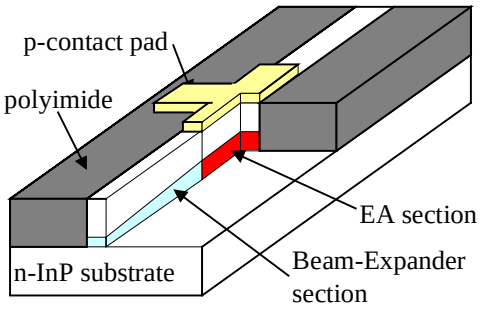

Fig.1 Schematic cross-section of the EA modulator with beam-expanders.

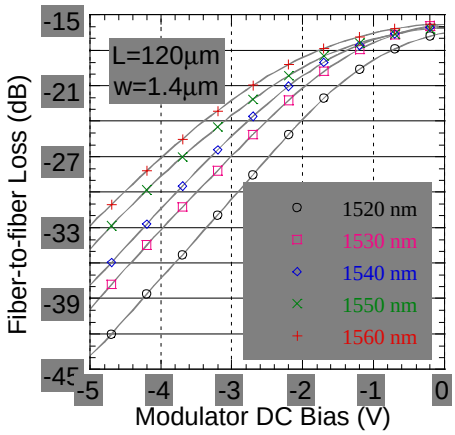

Fig.2 DC Extinction curves at different wavelengths.

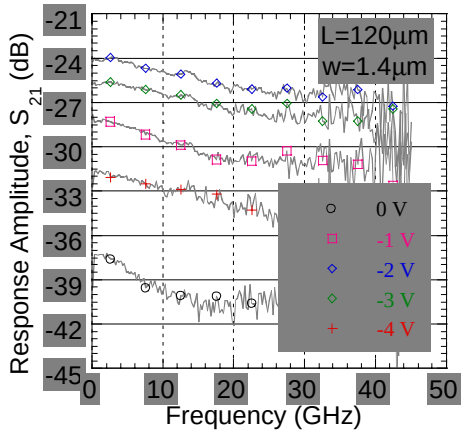

Fig.3 The Small-signal response curves of EA at different DC biases.

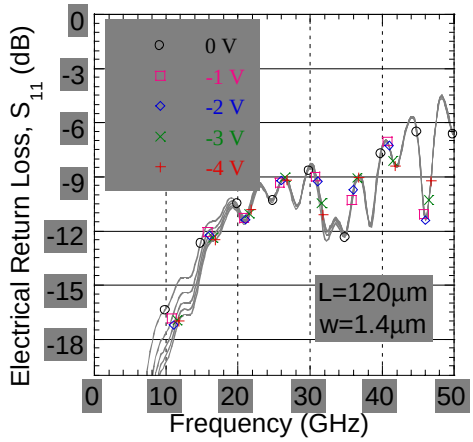

Fig.4 Electrical return loss of EA at different DC biases.

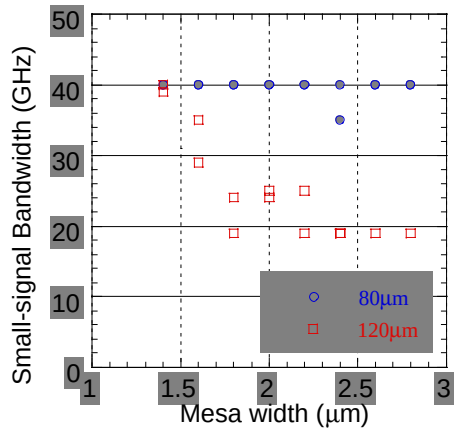

Fig.5 Small-signal modulation bandwidth as a function of the mesa width for two different EA lengths. The value 40 means the bandwidth is in excess of 35GHz, but could not be measured accurately.

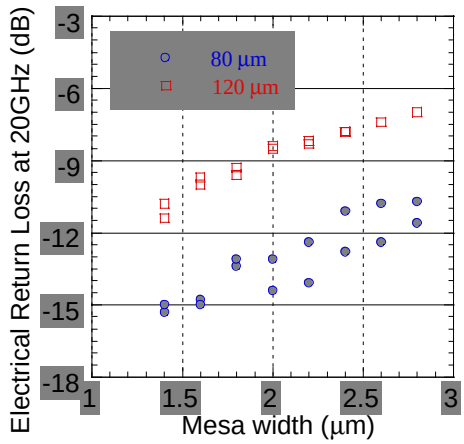

Fig.6 Electrical return loss at 20GHz as a function of the mesa width for two different EA lengths.